AN APPLICATION OF RECIPROCITY TO THE NUMERICAL MODELING OF A GPR SYSTEM

Michael McFadden and Waymond R. Scott, Jr.

Georgia Institute of Technology, School of Electrical and Computer Engineering

Atlanta, GA

m.mcfadden@gatech.edu, waymond.scott@ece.gatech.edu

ABSTRACT

In this paper, a technique is developed to model ground penetrating radar interactions. It combines reciprocity with the results from a full numerical model and allows one to compute a large number of scattering responses simultaneously provided the scatterers are small. The results of an example calculation are shown and compared with a full numerical model.

1. INTRODUCTION

In antenna engineering, reciprocity is used to compute the reception properties of an antenna from its transmission properties or vice versa. Reciprocity is implicitly invoked regularly in radar applications when the gain of an antenna is related to its effective aperture as a receiver. Both concepts are only useful for describing a radar interaction when the scatterer is in the far-field of the antenna. Because ground-penetrating radar (GPR) systems often interact with a scatterer in the near-field of the antennas, the use of reciprocity is less common, and often unjustified when invoked. In this paper, it is shown that for particular classes of scatterers, reciprocity can still be useful when characterizing and modeling a GPR system.

The GPR system studied in this paper is a two-antenna spiral-based system that has been built and modeled using the finite-difference time-domain method. Details of the system and the verification of the model are shown in [1]. In this system, the GPR is scanned over the ground along a lane that might contain a buried scatterer while radar measurements are taken periodically. When modeling a scan-lane response to a particular scatterer at some location, the numerical model must be run once for each location of the antennas above the ground. To characterize the system for different scatterer positions, one must run the model once for each combination of antenna location and scatterer location. Because the run-time of the simulation is on the order of hours, this can be very computationally burdensome.

To reduce the computation time, the proposed method is to treat the scattering interaction as three sub-problems in a similar way to an analytical treatment. To compute the scattered response on the antenna from some object, first the incident field on

This work was supported by the U.S. Army Engineer Research and Development Center Near-Surface Phenomenology Program under Contract 912HZ-07-C-0026

the scatterer is computed. Next, the induced currents are calculated from these incident fields. Finally, the received voltage obtained from the induced current is computed. By restricting the scatterers of interest to electrically small metallic objects and invoking reciprocity, each of the sub-problems can be solved using only two numerical simulations. With each problem solved in the general case, these two simulations allow one to obtain the scattered response from a small scatterer with an arbitrary geometry located at any position in the numerical grid.

In section 2, the relationship between the incident field and the induced current on a small scatterer is briefly described. Next, the reciprocity relation that allows one to quickly compute the received voltage for a given induced current is provided. In section 3, the derived relation is tested against the complete numerical model and is shown to give nearly identical results for a sufficiently small scatterer.

2. RECIPROCITY MODEL FOR A SMALL SCATTERER

In this section, an expression for the scattered voltage measured by a GPR system interacting with a small metallic scatterer is given. The expression allows the scattered voltage to be computed for an object anywhere in the numerical grid using two simulations of the antenna system. On the top of Fig. 1a, a generic two-antenna GPR system is shown with each antenna fed by a transmission line. In standard operation, the 1 antenna transmits a pulse and both the 1 and 2 antennas receive a response.

When the antennas are located at a position $\vec{r_a}$, and there is no buried scatterer present, a waveform, $V_{inc}(t)$, applied to the j antenna induces an incident electric field, $\vec{E}_j^I(t, \vec{r_a}, \vec{r})$, at a time t and position $\vec{r}$ in the space. Using the FDTD method, this field can be computed as a function of t over a range of $\vec{r}$ near the antennas using one simulation. When a scatterer is located near $\vec{r_s}$, a scattered current is induced, $\vec{J}_j^S(t, \vec{r_a}, \vec{r_s}, \vec{r})$, with support on the volume of the scatterer, U.

The scattered current distribution is, in general, a complicated function of the location of the antennas, and the location and geometry of the scattering object. However, by restricting interest only to electrically small metallic scatterers, one can easily compute the scattered current from the incident electric field vector at the scatterer's location, $\vec{E}_j^I(t, \vec{r_a}, \vec{r_s})$.

When a small scatterer interacts with an electric field, it is common to assume the induced charge distribution is some dipole that is a function of the incident field [2]. When considered in the frequency domain, this induced dipole is linearly related to the incident field, and the scatterer's geometry can consequently be modeled using a polarizability dyad, $\bar{\bar{\alpha}}$, with units of m^3. The current on the scatterer can then be related to the induced dipole moment using the continuity equation,

$$\vec{\mathbf{J}}_j^S(\omega, \vec{r_a}, \vec{r_s}, \vec{r}) = \mathbf{j}\omega\epsilon\bar{\bar{\alpha}} \cdot \vec{\mathbf{E}}_j^I(\omega, \vec{r_a}, \vec{r_s})\delta(\vec{r} - \vec{r_s}), \tag{1}$$

where the Fourier transform at ω is denoted in boldface, $\mathbf{j} = \sqrt{-1}$, and ϵ is the permittivity surrounding the scatterer.

When the scatterer is not present, a voltage is received on each antenna, i, of $V_{ij}^I(t, \vec{r_a})$. When the scatterer is present, an additional voltage, V_{ij}^S, is received. This is depicted in the middle of Fig. 1a. The total voltage is

$$V_{ij}^T(t, \vec{r_a}, \vec{r_s}) = V_{ij}^I(t, \vec{r_a}) + V_{ij}^S(t, \vec{r_a}, \vec{r_s}). \tag{2}$$

In general in GPR, the signal of interest for a scatterer is V_{ij}^S. The signal V_{ij}^I is typically calibrated out of the measurements by directly measuring the response obtained when no scatterer is present. For a known induced current distribution, a reciprocity relation can make the computation of the scattered voltage from a given induced current much easier. The expression for this

is an application of the Lorentz reciprocity relation and is obtained from a combination of arguments used in [3, 4]. The full argument is provided in [5]. The resulting equation provides the scattered voltage received on an antenna caused by a current distribution when the incident field created by that antenna is known,

$$\mathbf{V}_{ij}^{S}(\omega,\vec{r_a},\vec{r_s}) = -\frac{Z_0}{2\mathbf{V}_{inc}(\omega)}\iiint_U \left(\vec{\mathbf{E}}_i^{I}(\omega,\vec{r_a},\vec{r})\cdot\vec{\mathbf{J}}_j^{S}(\omega,\vec{r_a},\vec{r_s},\vec{r})\right)d\vec{r}, \tag{3}$$

where Z_0 is the characteristic impedance of the transmission line that feeds both antennas.

Using the assumed current distribution for a small scatterer at $\vec{r_s}$, (1), one concludes,

$$\mathbf{V}_{ij}^{S}(\omega,\vec{r_a},\vec{r_s}) = -\frac{\mathbf{j}\omega Z_0\epsilon}{2\mathbf{V}_{inc}(\omega)}\left(\vec{\mathbf{E}}_i^{I}(\omega,\vec{r_a},\vec{r_s})\cdot\bar{\bar{\alpha}}\cdot\vec{\mathbf{E}}_j^{I}(\omega,\vec{r_a},\vec{r_s})\right). \tag{4}$$

In this form, the scattered voltages, V_{ij}^{S}, for a small scatterer with any geometry characterized by $\bar{\bar{\alpha}}$ at any position $\vec{r_s}$ can be computed knowing the two field solutions, $\vec{E}_1^{I}$ and $\vec{E}_2^{I}$. Each can be obtained using one numerical simulation. In the next section, the reciprocity model derived here is verified against the full numerical simulation.

3. VERIFICATION OF RECIPROCITY MODEL

In this section, the reciprocity model shown in section 2 is tested by comparison with a full FDTD model. The GPR system modeled here is that described in [1] and a diagram of the system is shown at the bottom of Fig. 1a. The sand is modeled with a simple dielectric half-space of $\epsilon_r = 2.35$. A simulation is run where the 1 antenna transmits a pulse in the presence of a small wire. The $\vec{r_s}$ of the wire varies over the five points shown under the 1 antenna in the bottom of Fig. 1a. The scattered voltages, $V_{i1}^{S}(t,\vec{r_a},\vec{r_s})$ are obtained in the simulations for $i = 1, 2$ by running a calibration simulation with no dipole present to obtain V_{i1}^{I} and taking the difference from V_{i1}^{T}.

To compare with the reciprocity model in section 2, the fields in two simulations where no dipole is present are taken, $\vec{E}_j^{I}(t,\vec{r_a},\vec{r_s})$. The geometry of the small wire is encoded in the dyad, $\bar{\bar{\alpha}}$. This can be found analytically using [6],

$$\bar{\bar{\alpha}} = \frac{4\pi h^3\hat{\mathbf{y}}\hat{\mathbf{y}}}{3\left[\ln(2h/a)-1\right]}, \tag{5}$$

where for the dipole used, $a = 0.8$ mm is the radius, and $h = 1$ cm is half the height.

This provides all of the information necessary to compute $\mathbf{V}_{ij}^{S}$ using (4). Inverse Fourier transforming $\mathbf{V}_{i1}^{S}$, one obtains the time-domain responses of the wire, V_{i1}^{S}, which can be compared with the results computed by the full model. Comparisons are shown in Fig. 1b and 1c and show excellent agreement over all dipole positions tested. In the figures, all V_{21}^{S} have been scaled up by a factor of 75 times compared with the V_{11}^{S} measurements.

4. CONCLUSIONS

A model of a GPR system based on the use of a numerical model and reciprocity has been presented. The model shows excellent agreement with a complete numerical model, but has the advantage of computing a large number of scattering interactions simultaneously using only two numerical simulations. Comparisons are shown to the full model for a small dipole scatterer and good agreement is found even when the scatterer is very near the transmitting antenna or the air-ground interface. Several applications for the model are possible, including GPR system analysis and imaging methods.

Due to space limitations, this abstract does not contain a measured verification of the reciprocity model. In the full paper, measured data from two small scatterers will be compared directly with the reciprocity model prediction. A discussion of the differences between symmetric target and asymmetric target responses will be provided.

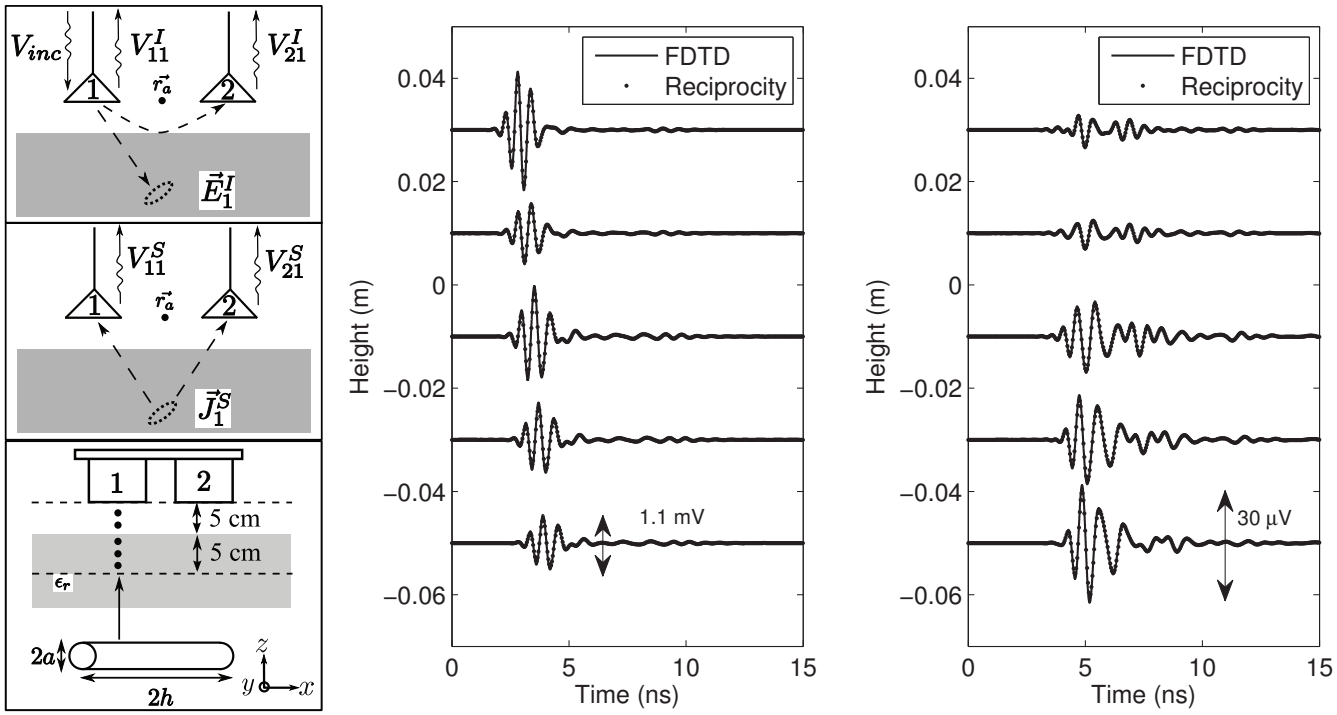

Fig. 1. (a) The top two show configurations of a generic GPR. The bottom shows the verification test. (b) $V_{11}^S(t)$ responses. (c) $V_{21}^S(t)$ responses. (b) and (c) show full FDTD and reciprocity predictions of the scattered response seen from a small dipole at positions shown at the bottom of (a). Heights are measured in the z direction with zero at the air-ground interface.

5. REFERENCES

[1] M. McFadden and W. R. Scott, Jr., "Numerical Modeling of a Spiral-antenna GPR System," in *IEEE International Geoscience and Remote Sensing Symposium*, Honolulu, HI, June 2009.

[2] C. E. Baum, *Detection and Identification of Visually Obscured Targets*. Taylor and Francis, 1999, ch. 6, pp. 166–169.

[3] R. S. Elliott, *Antenna Theory and Design*. Wiley Interscience, 2003, ch. 1, pp. 38–52.

[4] R. Azaro, S. Caorsi, and M. Pastorino, "On the Relationship For the Monostatic Modulated Fundamental Scattering Technique," *Microwave and Optical Letters*, vol. 38, pp. 187–190, 2003.

[5] M. McFadden, "Analysis of The Equiangular Spiral Antenna," Ph.D. dissertation, Georgia Inst. Tech., 2009.

[6] G. S. Smith, *Classical Electromagnetic Radiation*. Cambridge, 1997, ch. 7, pp. 516–519.